PHYSICAL REVIEW A VOLUME 45, NUMBER 7 1 APRIL 1992

Experimental observation of enhanced nonresonant nonlinear optical responses from optically pumped electronic excited states

J. R. Heflin, D. C. Rodenberger, R. F. Shi, M. Wu, N. Q. Wang, Y. M. Cai, and A. F. Garito
Department of Physics, University of Pennsylvania, Philadelphia, Pennsylvania 19104
(Received 24 October 1991)

Enhancement of greater than 2 orders of magnitude of nonresonant third-harmonic generation from an optically pumped S_1 electronic excited state is experimentally observed for quasi-two-dimensional conjugated disklike structures. The isotropically averaged S_1 excited-state microscopic susceptibility $\langle\gamma^{S_1}(-3\omega;\omega,\omega,\omega)\rangle$ is $-1640\pm100\times10^{-36}$ esu, and the corresponding macroscopic $\chi^{(3)}_{S_1}(-3\omega;\omega,\omega,\omega)$ exhibits temporal decay and pump-power saturation behavior associated with the expected decay and saturation of the S_1 state. The enhancement mechanism through optical pumping followed by a nonresonant nonlinear optical probe is generalizable to both second- and third-order optical processes in nonlinear optical media.

PACS number(s): 42.50.−p, 78.47.+p, 42.65.−k

In nonresonant nonlinear optical processes in electronic systems, the real population of the initial state for the virtual optical excitations can be either the usual singlet ground state S_0 or an optically pumped excited state S_n. In earlier theoretical studies [1,2] of microscopic third-order optical susceptibilities $\gamma_{ijkl}(-\omega_4;\omega_1,\omega_2,\omega_3)$ of quasi-one- (1D) and quasi-two-dimensional (2D) chainlike and disklike conjugated structures, we found that, compared to the ground state [3,4], nonresonant $\gamma_{ijkl}(-\omega_4;\omega_1\omega_2,\omega_3)$ susceptibilities can markedly increase, or even change sign, when the first (S_1), or second (S_2), π-electron excited state is optically pumped and then populated on time scales sufficiently long to allow nonresonant measurements of $\gamma^{S_n}_{ijkl}(-\omega_4;\omega_1,\omega_2,\omega_3)$. The principal reasons are the larger optical transition moments $\mu_{nn'}$ and smaller excitation energies $\omega_{nn'}$ between excited states S_n and $S_{n'}$, especially for highly charge correlated virtual excitations, and a reduced degree of competition between virtual excitation processes that contribute with opposite signs to determine the magnitude, sign, and dispersion of $\gamma_{ijkl}(-\omega_4;\omega_1,\omega_2,\omega_3)$ [2]. The electron-correlation microscopic origin of the ground state $\gamma_{ijkl}(-\omega_4;\omega_1,\omega_2,\omega_3)$ has been experimentally confirmed through a series of dc-induced second-harmonic generation (DCSHG) and third-harmonic generation (THG) dispersion measurements of key conjugated linear-chain structures [5]. In this paper, we report the experimental observation that the nonresonant $\gamma_{ijkl}(-3\omega;\omega,\omega,\omega)$ is enhanced by orders of magnitude when the S_1 π-electron excited state of a disklike conjugated structure is populated for nanosecond time scales and then probed nonresonantly through THG with time-delayed picosecond pulses. THG was selected as the probe process because of its exclusive electronic origin as compared to, say, degenerate four-wave mixing (DFWM), which has multiple contributions to the nonlinear optical response.

The nonlinear optical medium, silicon naphthalocyanine (SINC) [4,6], exhibits characteristic large oscillator strength Q [$\lambda=778$ nm (1.59 eV)] and B (Soret) [$\lambda=335$ nm (3.70 eV)] absorption bands due to widely separated S_0 (1^1A_{1g})$\rightarrow S_1(1^1E_u)$ and S_0 (1^1A_{1g})$\rightarrow S_2(2^1E_u)$ π-electron transitions, respectively, as is well-established for diamagnetic metallophthalocyanines and related metalloporphyrins of D_{4h} symmetry [7,8]. Importantly, we have previously demonstrated that SINC exhibits absorption saturation of the $S_0\rightarrow S_1$ transition and behaves as an optical Bloch two-level system having a decay time of several nanoseconds [4]. Separate THG measurements [9] over the near-infrared region (1907–1064 nm) of the frequency-dependent, isotropically averaged, S_0 ground state $\langle\gamma^{S_0}(-3\omega;\omega,\omega,\omega)\rangle$ of SINC solutions show that for 10-ns pulses of fundamental wavelength $\lambda=1543$ nm, well below the $S_0\rightarrow S_1$ Q band, $\langle\gamma^{S_0}(-3\omega;\omega,\omega,\omega)\rangle$ is relatively small, being less than the experimental uncertainty of $\pm10\times10^{-36}$ esu. The created third harmonic at 514 nm lies in the transparency window between the $S_0\rightarrow S_1$ and $S_0\rightarrow S_2$ absorption bands.

The excited-state THG measurements in the present study were performed on dilute solutions of SINC dissolved in transparent dioxane [$C=(1-5)\times10^{-4}$ moll^{-1}] using the Maker fringe method in a flow cell wedged configuration. The laser source was a 10-Hz, 30-ps pulse width, mode-locked Nd:YAG laser (YAG denotes yttrium aluminum garnet) with 40-mJ/pulse output at a wavelength of 1064 nm. The nonresonant probe beam at 1543 nm and the pump beam at 770 nm (in the $S_0\rightarrow S_1$ Q absorption band) were created, respectively, by focusing the 1064-nm laser output and its 532-nm second harmonic, generated in a potassium dihydrogen phosphate doubling crystal, into two separate methane Raman cells. The 770-nm pump beam passes through a right-angle prism employed as a retroreflector and mounted on a 1-m-long translation stage that enables temporal delay of the two beams. The 1543-nm probe beam is beamsplit with one arm focused on a glass plate that serves as a reference to divide out power fluctuations and with the other focused on the sample cell. TH light at 514 nm is detected by photomultiplier tubes in each arm after frequency selection by spike and bandpass filters.

The sample cell consists of two 5-cm-long BK-7 glass

windows mounted to form a wedge compartment with angle $\alpha=0.0123$ rad and mean thickness 0.44 mm and is located on a computer-controlled, stepper motor-driven translation stage where the translational axis is perpendicular to the direction of beam propagation [5,10]. The 770-nm pump beam intersects the 1543-nm probe beam in the center of the cell at an angle of 7°, and the overlapping and focal point coincidence of the two beams are carefully adjusted.

The TH fringes were analyzed to obtain $\chi_S^{(3)}(-3\omega;\omega,\omega,\omega)$ of the sample according to the expression

$$\chi_S^{(3)}=\frac{n_{3\omega}^S+n_\omega^S}{l_c^S T_S (t_S^{(2)})^3}\left[T_{GS}\frac{l_c^G\chi_G^{(3)}}{n_{3\omega}^G+n_\omega^G}+\left(\frac{\bar{A}^S}{\bar{A}^R}\right)^{1/2}\left|T_{GR}\frac{l_c^G\chi_G^{(3)}}{n_{3\omega}^G+n_\omega^G}-T_R\frac{l_c^R\chi_R^{(3)}}{n_{3\omega}^R+n_\omega^R}(t_R^{(2)})^3\right|\right], \tag{1}$$

where $\bar{A}^S$ and $\bar{A}^R$ are the mean fringe amplitudes of the sample and reference liquids, respectively, l_c is the coherence length, T_{AB} and t_A are transmission factors for the glass-liquid interfaces, and the subscript G refers to the BK-7 glass windows [5]. For the reference liquid, pure dioxane, we obtain $\chi^{(3)}(-3\omega;\omega,\omega,\omega)=0.702\times10^{-14}$ esu and $l_c=19.6$ μm, and for the glass windows we use the values $\chi^{(3)}(-3\omega;\omega,\omega,\omega)=0.600\times10^{-14}$ esu and $l_c=13.03$ μm [5]. The coherence length l_c remained constant and the TH intensity was cubic in fundamental intensity for all measured concentrations of SINC both with and without the pump beam.

Although SINC molecules occupying the ground state have negligible absorption at 1543 and 514 nm, we have directly measured weak excited-state absorption (ESA) at both the fundamental and harmonic wavelengths [11]. A modified configuration of the excited-state THG measurement was used to characterize the ESA of SINC. Maintaining the alignment of the 770-nm pump beam, we directly detected the transmission of a 1543 or 532 nm (0.08 eV away from the third-harmonic wavelength 514 nm) probe beam focused into an overlapping position in the flowing sample. The magnitude of the ESA coefficient α_{S_1} is determined by the difference between overlapping and negative time delayed probe pulses with respect to the pump pulse by

$$\frac{I_2-I_1}{I_1}=\frac{e^{-\alpha_{S_1}l}-e^{-\alpha_{S_0}l}}{e^{-\alpha_{S_0}l}}\cong e^{-\alpha_{S_1}l}-1, \tag{2}$$

where I_2 is the transmitted probe beam intensity when the pump and probe temporally overlap, I_1 is the transmitted probe beam intensity when the probe precedes the pump, and the ground-state absorption coefficient α_{S_0} is negligible. The linear fits of values of α_{S_1} obtained as a function of SINC concentration result in experimental values for the molecular ESA cross section $\sigma_{S_1}=\alpha_{S_1}/N_{S_1}$ of 3.2 ± 0.3 and $4.7\pm0.5\times10^{-17}$ cm^2 at 1543 and 532 nm, respectively. These values are in good agreement with independent measurements of the intensity-dependent absorption of a single 532-nm beam through solutions of SINC in toluene that obtained $\sigma_{S_1}=3.9\times10^{-17}$ cm^2 [12]. We observed both transient and saturation behavior to verify the expected characteristics of the ESA signal. As an example, the decay of the ESA as a function of the time delay between the 770-nm pump and 532-nm probe is shown in Fig. 1. The effects of absorption on the Maker fringes are accounted for fully by using in Eq. (1) the corrected mean fringe amplitude $\bar{A}^S_{\rm corr}$ given by

$$\bar{A}^S_{\rm corr}=\frac{2\bar{A}^S_{\rm meas}}{e^{-3\alpha_\omega l}+e^{-\alpha_{3\omega}l}}, \tag{3}$$

where $\bar{A}^S_{\rm meas}$ is the directly measured mean fringe amplitude and α_ω ($\alpha_{3\omega}$) is the linear absorption coefficient of the sample at the fundamental (third harmonic) wavelength.

In solution, the macroscopic susceptibility $\chi^{(3)}(-3\omega;\omega,\omega,\omega)$ derives from the weighted sum of the isotropically averaged molecular susceptibilities $\langle\gamma(-3\omega;\omega,\omega,\omega)\rangle$ of each component. For SINC in dioxane where both the S_0 and S_1 states of SINC may have real populations, $\chi^{(3)}(-3\omega;\omega,\omega,\omega)$ is given by

$$\chi^{(3)}(-3\omega;\omega,\omega,\omega)=(f^\omega)^3 f^{3\omega}[N_D\langle\gamma^D(-3\omega;\omega,\omega,\omega)\rangle+N_{S_0}\langle\gamma^{S_0}(-3\omega;\omega,\omega,\omega)\rangle+N_{S_1}\langle\gamma^{S_1}(-3\omega;\omega,\omega,\omega)\rangle], \tag{4}$$

where N_D, N_{S_0}, and N_{S_1} are the number densities of dioxane molecules and SINC molecules occupying the S_0 and S_1 states, respectively, and we have assumed the local field factors f^ω are the same for each component. Figure 2 shows typical examples of TH fringes obtained both with and without the 770-nm pump beam resonantly exciting the $S_0\rightarrow S_1$ transition at a fixed probe delay of 20 ps. At relatively low concentrations, optical pumping of S_1 leads to greater than 60% reduction in the TH fringe amplitude. In agreement with our previous nanosecond THG measurements of $\langle\gamma^{S_0}(-3\omega;\omega,\omega,\omega)\rangle$ [9], the unpumped Maker fringes and $\chi^{(3)}(-3\omega;\omega,\omega,\omega)$ values are found to be independent of concentration, demonstrating that $\gamma^{S_0}(-3\omega;\omega,\omega,\omega)$ is so small that the term $N_{S_0}\langle\gamma^{S_0}(-3\omega;\omega,\omega;\omega)\rangle$ of Eq. (4) is negligible. Since $N_{S_1}=0$ in the unpumped configuration, the unpumped TH fringe shown in Fig. 2 originates purely from the dioxane term $N_D\langle\gamma^D(-3\omega;\omega,\omega,\omega)\rangle$.

The large decrease in TH fringe amplitude in Fig. 2 when the S_1 state is optically pumped is due to a very large $\langle\gamma^{S_1}(-3\omega;\omega,\omega,\omega)\rangle$ that is of opposite sign to $\langle\gamma^D(-3\omega;\omega,\omega,\omega)\rangle$ leading to a reduction of $\chi^{(3)}(-3\omega;\omega,\omega,\omega)$ for the solution as a whole. Accordingly, in sharp contrast to the unpumped case, the pumped $\chi^{(3)}(-3\omega;\omega,\omega,\omega)$ values shown in Fig. 3 are observed to decrease dramatically with concentration when SINC is resonantly pumped at 770 nm and the S_1 state is populated. The linear fit in Fig. 3 yields $\chi_{S_1}^{(3)}(-3\omega;\omega,\omega,\omega)/C=-(1.55\pm0.09)\times10^{-12}$ esu l mol^{-1} where

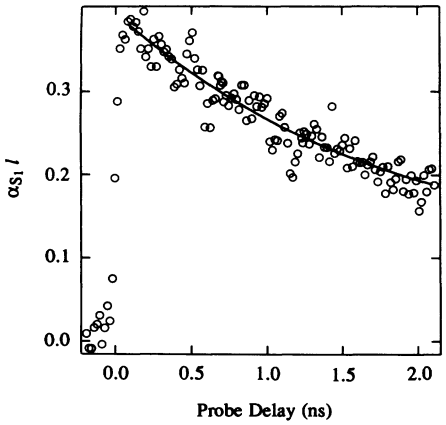

FIG. 1. Excited-state absorption at 532 nm of SINC dissolved in dioxane as a function of the delay between the 532-nm probe and 770-nm pump pulses. The solid curve fit to the data yields an S_1 lifetime of $\tau = 1.8 \pm 0.3$ ns.

$$\chi^{(3)}_{S_1}(-3\omega;\omega,\omega,\omega) = \chi^{(3)}_{\text{pump}}(-3\omega;\omega,\omega,\omega) - \chi^{(3)}_{\text{no pump}}(-3\omega;\omega,\omega,\omega)$$

is the contribution of the excited state to the overall $\chi^{(3)}(-3\omega;\omega,\omega,\omega)$ and C is the molar concentration. From the relation

$$\chi^{(3)}_{S_1}(-3\omega;\omega,\omega,\omega) = \tfrac{1}{2} N_0 (f^{\omega})^3 f^{3\omega} \langle \gamma^{S_1}(-3\omega;\omega,\omega,\omega)\rangle \tag{5}$$

where N_0 is the number density of SINC molecules, $N_0/2$ is the excited-state population of a two-level system for $I \gg I_S$, and $f^{\omega} = (n_{\omega}^2+2)/3$ is the Lorentz-Lorenz local field factor, we obtain $\langle \gamma^{S_1}(-3\omega;\omega,\omega,\omega)\rangle = -(1640 \pm 100) \times 10^{-36}$ esu. Thus, the real population of the S_1 state by optical pumping increases $\langle \gamma(-3\omega;\omega,\omega,\omega)\rangle$ of SINC by greater than 2 orders of magnitude. For comparison, the measured value of $\langle \gamma(-3\omega;\omega,\omega,\omega)\rangle$ for hexatriene, an $N=6$ carbon site linear chain, is 1.2×10^{-36} esu at $\lambda = 1543$ nm while the values for β carotene, an $N=22$ site chain possessing a very large third-order susceptibility, are 52×10^{-36} esu at the nonresonant wavelength $\lambda = 2148$ nm and 358×10^{-36} esu at the near-resonant wavelength $\lambda = 1543$ nm [5].

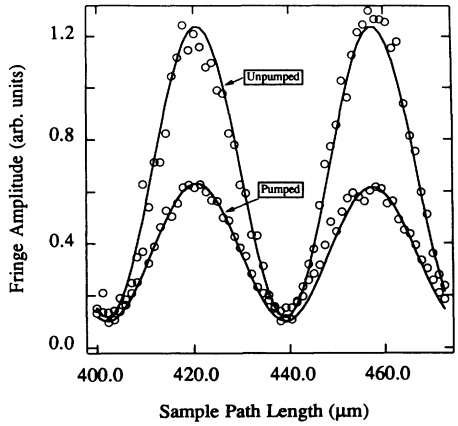

FIG. 2. Third-harmonic fringes of SINC in dioxane at 514 nm both with and without the 770-nm pump beam resonantly populating the S_1 state. For pure dioxane, the fringes are identical to those for the unpumped configuration. The large decrease in fringe amplitude in the pumped configuration results from a very large, negative $\langle \gamma^{S_1}(-3\omega;\omega,\omega,\omega)\rangle$.

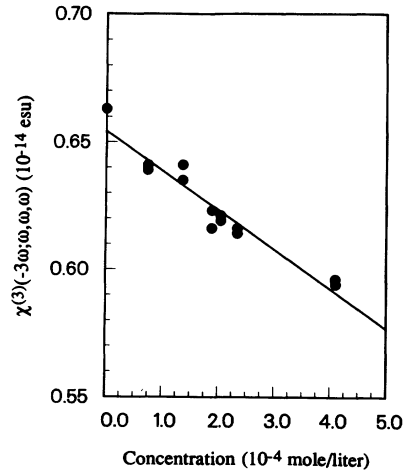

FIG. 3. Concentration dependence of $\chi^{(3)}(-3\omega;\omega,\omega,\omega)$ for solutions of SINC in dioxane in the pumped configuration. The linear fit to the data yields $\langle \gamma^{S_1}(-3\omega;\omega,\omega,\omega)\rangle = -1640 \pm 100 \times 10^{-36}$ esu compared to $|\langle \gamma^{S_0}(-3\omega;\omega,\omega,\omega)\rangle| < 10\times10^{-36}$ esu. Each measured value of $\chi^{(3)}(-3\omega;\omega,\omega,\omega)$ has an associated uncertainty of $\pm 15\%$ determined from the reproducibility of the Maker fringes and from uncertainties in the standard and derived values employed for BK-7 glass and dioxane.

As the S_1 excited-state population spontaneously decays back to the S_0 state, $\chi^{(3)}_{S_1}(-3\omega;\omega,\omega,\omega)$ is expected to decrease and approach zero in the limit $t \gg \tau$, where τ is the decay time of S_1. In the limit of negligible S_0 ground-state contribution to $\chi^{(3)}(-3\omega;\omega,\omega,\omega)$, $\chi^{(3)}_{S_1}(-3\omega;\omega,\omega,\omega)$ is directly proportional to the S_1 population and is therefore expected to decay as $e^{-t/\tau}$. This was verified by adjusting the relative delay between the pump and probe beams as shown in Fig. 4. As expected, when the probe precedes the pump, $\chi^{(3)}_{S_1}(-3\omega;\omega,\omega,\omega) = 0$, and the width of the rising edge of the signal is in accordance with the 30-ps laser pulse width. This is followed by an exponential decay of $\chi^{(3)}_{S_1}(-3\omega;\omega,\omega,\omega)$ as the probe beam encounters a partially decayed S_1 population. The inset of Fig. 4 illustrates $\ln|\chi^{(3)}_{S_1}(-3\omega;\omega,\omega,\omega)|$ versus probe delay. The excellent linear fit yields $\tau = 1.50 \pm 0.05$ ns in agreement with our own separate spectral measurements of τ shown in Fig. 1 and other independent results [8,13]. The data of Fig. 4 rule out both nonlinear beam interaction and thermal effects as sources for the decrease of $\chi^{(3)}(-3\omega;\omega,\omega,\omega)$ when the sample is pumped.

The steady-state solution to the population rate equations for a simple two-level system involving states S_0 and S_1 yields $N_{S_1} = N_0 I/2(I+I_S)$ where the saturation intensity $I_S = \hbar\omega/2\sigma\tau$, σ is the absorption cross section for the $S_0 \rightarrow S_1$ transition, and τ is the S_1 state lifetime [14]. The saturation of the $\chi^{(3)}_{S_1}(-3\omega;\omega,\omega,\omega)$ signal with increased pump intensity is well fit by a function of the form

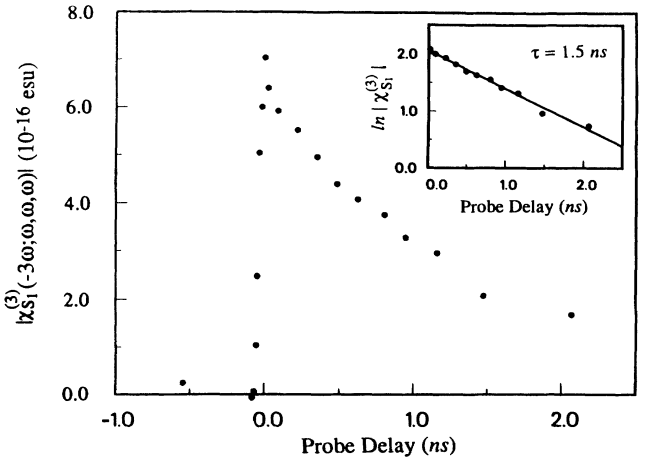

FIG. 4. $\chi^{(3)}_{S_1}(-3\omega;\omega,\omega,\omega)$ as a function of the time delay between the pump and probe beams. As shown in the inset, the data are well fit by a decay $e^{-t/\tau}$ with an S_1 lifetime of $\tau = 1.50 \pm 0.05$ ns.

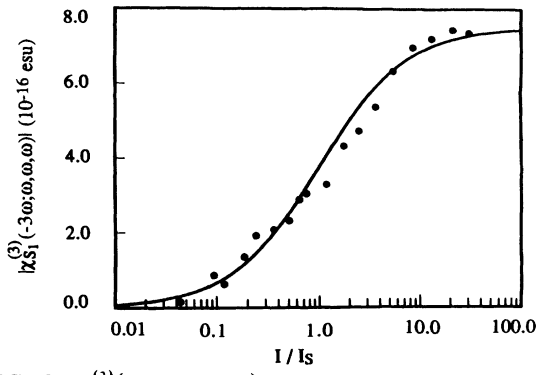

FIG. 5. $\chi^{(3)}_{S_1}(-3\omega;\omega,\omega,\omega)$ as a function of relative pump beam intensity I/I_S. The saturation of $\chi^{(3)}_{S_1}(-3\omega;\omega,\omega,\omega)$ is due to a saturation of the S_1 state population. The solid curve is a fit of the form $\chi^{(3)}_{S_1}(-3\omega;\omega,\omega,\omega) \propto I/(I+I_S)$ based on the population rate equations of a two-level system. The probe delay was fixed at 20 ps.

$I/(I+I_S)$ in Fig. 5 in agreement with saturation of the S_1 state population.

In summary, we have observed an enhancement of the nonresonant molecular third-harmonic susceptibility $\langle\gamma(-3\omega;\omega,\omega,\omega)\rangle$ by more than 2 orders of magnitude upon optical pumping of the designated S_1 state of a conjugated disklike structure SINC. A unique experimental configuration was employed in which the nonlinear optical medium is first optically excited with a pump beam resonant with an electronic transition and then probed with a time-delayed nonresonant beam via third-harmonic generation. When SINC solutions were resonantly pumped, $\chi^{(3)}(-3\omega;\omega,\omega,\omega)$ was observed to decrease dramatically and to further decrease linearly with increased concentration because the excited state $\langle\gamma^{S_1}(-3\omega;\omega,\omega,\omega)\rangle$ is negative in sign and orders of magnitude larger than the ground state $\langle\gamma^{S_0}(-3\omega;\omega,\omega,\omega)\rangle$. The contribution of the S_1 state to the macroscopic third-order susceptibility $\chi^{(3)}_{S_1}(-3\omega;\omega,\omega,\omega)$ was found to decay with the S_1 state lifetime and saturate at high pump intensities in accordance with the expected decay and saturation of the S_1 state population. The enhancement mechanism for nonlinear optical responses reported here is generalizable to both third-order $\chi^{(3)}(-\omega_4;\omega_1,\omega_2,\omega_3)$ and second-order $\chi^{(2)}(-\omega_3;\omega_1,\omega_2)$ optical processes and to other material structures, compositions, and phases.

This research was generously supported by AFOSR and DARPA (Grant No. F49620-85-C-0105), Penn Research Fund, Pittsburgh Supercomputing Center, and partially by NSF/MRL (Grant No. DMR-85-19059). We gratefully acknowledge the contribution of C. Yan and many stimulating discussions with Dr. K. Y. Wong.

[1] A. F. Garito, in *Proceedings of the Optical Society of America Annual Meeting, 1989,* Technical Digest Series, Vol. 18 (Optical Society of America, Washington, DC, 1989), p. 22.

[2] Q. L. Zhou, J. R. Heflin, K. Y. Wong, O. Zamani-Khamiri, and A. F. Garito, Phys. Rev. A **43**, 1673 (1991).

[3] J. R. Heflin, K. Y. Wong, O. Zamani-Khamiri, and A. F. Garito, J. Opt. Soc. Am. B **4**, 136 (1987); Phys. Rev. B **38**, 1573 (1988).

[4] J. W. Wu, J. R. Heflin, R. A. Norwood, K. Y. Wong, O. Zamani-Khamiri, A. F. Garito, P. Kalyanaraman, and J. Sounik, J. Opt. Soc. Am. B **6**, 707 (1989), and references therein.

[5] J. R. Heflin, Y. M. Cai, and A. F. Garito, J. Opt. Soc. Am. B **8**, 2132 (1991).

[6] B. L. Wheeler, G. Nagasubramanian, A. J. Bard, L. A. Schectman, D. R. Dininny, and M. E. Kenney, J. Am. Chem. Soc. **106**, 7404 (1984).

[7] See, for example, M. Gouterman, in *The Porphyrins,* edited by D. Dolphin (Academic, New York, 1978), Vol. 3, Chap. 1.

[8] W. F. Kosonocky and S. E. Harrison, J. Appl. Phys. **37**, 4789 (1966).

[9] N. Q. Wang, Y. M. Cai, J. R. Heflin, and A. F. Garito, Mol. Cryst. Liq. Cryst. **189**, 39 (1990). The values for $\langle\gamma(-3\omega;\omega,\omega,\omega)\rangle$ reported in this paper use a reference standard value that is 8.0 times larger than the one employed in the present work. See Ref. [5] for details.

[10] F. Kajzar and J. Messier, Phys. Rev. A **32**, 2352 (1985); Rev. Sci. Instrum. **58**, 2081 (1987), and references therein.

[11] D. C. Rodenberger and A. F. Garito, *Quantum Electronics and Laser Science,* 1991 Technical Digest Series (Optical Society of America, Washington, DC, 1991), p. 188.

[12] J. W. Perry *et al.*, in *Organic Molecules for Nonlinear Optics and Photonics,* edited by J. Messier *et al.* (Kluwer Academic, Dordrecht, 1991), p. 369.

[13] A Kaltzbeitzel, D. Neher, C. Bubek, T. Sauer, G. Wegner, and W. Caseri, in *Electronic Properties of Conjugated Polymers,* edited by H. Kuzmany, M. Mehring, and S. Roth (Springer, New York, 1989); and A. Kaltzbeitzel, Ph.D. dissertation, University of Mainz, 1989 (unpublished).

[14] See, for example, A. E. Siegman, *Lasers* (University Science Books, Mills Valley, CA, 1986), pp. 204–206.